Journal of Non-Newtonian Fluid Mechanics 317 (2023) 105056

Contents lists available at ScienceDirect

Journal of Non-Newtonian Fluid Mechanics

journal homepage: www.elsevier.com/locate/jnnfm

Entrance length estimates for flows of power-law fluids in pipes and channels

Chryso Lambride [a], Alexandros Syrakos [a], Georgios C. Georgiou [b,*]

[a] Department of Mechanical and Manufacturing Engineering, University of Cyprus, PO Box 20537, 1678, Nicosia, Cyprus
[b] Department of Mathematics and Statistics, University of Cyprus, PO Box 20537, 1678, Nicosia, Cyprus

ARTICLE INFO

Keywords:
Development length
Power-law fluid
Wall shear stress
Laminar flow
Pipe
Channel

ABSTRACT

The entrance length needed for pipe and channel flows to re-adjust from a uniform to a fully-developed velocity profile is typically defined as the length required for the centreline velocity to reach 99% of its fully-developed value. This definition may be quite inaccurate in non-Newtonian flows with almost flat fully-developed velocity distributions near the centreline. Shear-thinning and viscoplasticity may cause the flow close to the centreline to evolve faster than that closer to the walls. Thus, alternative definitions of the entrance length have been proposed, e.g., for viscoplastic flows.

In the present work, we numerically solve the flow development of power-law fluids in pipes and channels and calculate the entrance length as a function of the transverse coordinate, determining the global entrance length, L_g, along with the standard centreline estimate, L_c. We also consider an alternative definition, L_t, based on the evolution of the wall shear stress. Results have been obtained for values of the power-law exponent n ranging from 0.2 to 1.5 and for Reynolds numbers (Re) up to 1000. In pipes, centreline and global entrance lengths coincide for $n>0.7$, i.e., the flow indeed develops more slowly at the symmetry axis. This is not the case, however, with fluids that are more shear-thinning. Big differences are observed, which are more pronounced at lower Re. The stress entrance length is smaller than the classical centreline entrance length except for $n<0.4$ and $n>1.45$. More dramatic are the differences in channel flow. For $n<1$ (shear thinning fluids), L_c is smaller than both L_t and L_g. The differences are relatively reduced as Re and n are increased.

1. Introduction

Fluid particles steadily entering a long conduit, such as a circular pipe or a straight channel, at a uniform velocity eventually readjust to the fully-developed Poiseuille distribution far downstream at a distance known as the entrance or development length. Estimates of the latter length are very important in many applications, e.g., in the design of pipe networks, in transition-to-turbulence studies [1], in rheometry [2], in microfluidics [3], and in hemodynamics [4]. If the entrance length is small compared to the total length of a pipe (or a channel), then the assumption of Poiseuille flow can be employed in order to obtain reliable estimates of useful quantities in flows of industrial interest or in biofluid mechanics, such as the wall shear stress and the maximum velocity [4,5].

The development of the flow of a Newtonian fluid in a cylindrical tube or a channel has been extensively studied experimentally and computationally [6]. Approximate analytical solutions have also been derived [7]. The development or entrance length, L_c^*, is typically defined as the distance required for the maximum velocity at the axis or plane of symmetry to reach 99% of its fully-developed value, predicted by the corresponding Poiseuille's formula. This is usually scaled by the pipe diameter or the channel width [6]. Thus, the dimensionless development length for a tube of radius R^* is given by $L_c = L_c^*/(2R^*)$; similarly, $L_c = L_c^*/(2H^*)$ for a channel of semi-width H^*. It should be noted that throughout the paper, stars denote dimensional variables or parameters and are dropped for their corresponding dimensionless counterparts.

Most studies of Newtonian flow development arrived at correlations between the dimensionless development length L_c and the Reynolds number Re [1,6]. Kountouriotis et al. [8] studied the Newtonian development length problem in the presence of wall slip following Navier's slip equation, and introduced an alternative definition of the development length based on the slip velocity. Hence, the wall development length, L_w, has been defined as the length required for the slip velocity to decrease to 1.01% of its fully-developed value. Their

* Corresponding author.
E-mail address: georgios@ucy.ac.cy (G.C. Georgiou).

https://doi.org/10.1016/j.jnnfm.2023.105056
Received 21 October 2022; Received in revised form 18 March 2023; Accepted 19 April 2023
Available online 20 April 2023

numerical simulations in both channels and pipes showed that both L_c and L_w increase with wall slip passing through a maximum and vanish at a critical value of the slip parameter corresponding to the full-slip case [8]. An interesting finding was that the flow development is slower at the centreline only in the case of a pipe. In channels, the flow development is slower at the wall, which implies that $L_w > L_c$. Given that the slip velocity is generally an increasing function of the wall shear stress [9], this result motivates an alternative definition of the development length based on the wall shear stress, as discussed below.

In a later computational study of Newtonian entrance flow, Joshi and Vinoth [10] tried also an alternative ("streamtube") configuration where the uniform velocity inlet boundary condition is moved a distance upstream of the actual pipe or channel entrance, arguing that this is more realistic than setting the flat profile right at the pipe / channel entrance. They found that this reduces the development length at low Reynolds numbers compared to the classic configuration, while the effect is more limited at higher Reynolds numbers. They also calculated the "global" entrance length of Philippou et al. [11] (see below), and their results showed that the velocity development at some transverse location is slower than the centreline one in channels, whereas in pipes the flow development is slowest at the symmetry axis, in agreement with the findings of Kountouriotis et al. [8]. Finally, they defined also some entrance lengths based on integral quantities that are dependant on the velocity profile across the whole pipe or channel cross-section.

Most fluids of industrial, geophysical, and biological interest are non-Newtonian. Non-Newtonian behaviour includes shear thinning or shear thickening, viscoplasticity, viscoelasticity, and thixotropy. For example, blood exhibits each of the aforementioned rheological phenomena to some degree [12,13]. Its non-Newtonian character is predominant in small arteries and veins where the diameter is close to the size of red blood cells [14].

Studies of entrance flows of viscoplastic fluids, i.e., of fluids exhibiting yield stress, have demonstrated that the standard definition of the development length (L_c) is not representative of the actual length needed for the flow to develop fully across the tube or the channel. The flow near the centre of the pipe develops rapidly, especially at higher values of the yield stress, because once the unyielded plug has formed there, any further flow development is impossible. As was first pointed out by Vradis et al. [15], higher plasticity causes the solidified core, which moves with a uniform velocity, to spread closer to the walls, and therefore its velocity is closer to the inlet velocity, not requiring much readjustment. At the same time though, the flow nearer to the walls, where the fluid is yielded, continues to develop farther downstream. Therefore, a definition of the development length based on the maximum velocity is not appropriate. Ookawara et al. [16] introduced an alternative definition based on the velocity near the radial edge of the solidified plug at 95% of the plug radius (L_{95}). They also employed a modified definition of the Reynolds number in an effort to collapse the viscoplastic development-length-versus-*Re* curves onto the Newtonian one, for all values of the Bingham number. Later, Poole and Chhabra [17] obtained more detailed numerical results and showed that, while the viscoplastic development length curves can indeed collapse onto the Newtonian one at high Reynolds numbers under a suitable definition of *Re*, the same cannot happen at the low *Re* limit, where the Bingham number always differentiates between the curves. Georgiou and coworkers [11,18] examined the problem further, monitoring the development length as a function of the transverse coordinate, with and without wall slip. They found that neither L_c nor L_{95} are adequate definitions (in fact, not even in the Newtonian channel flow if wall slip is present), but instead proposed a global development length, L_g, which is the maximum development length across the pipe or channel. In a recent work, Dimakopoulos et al. [19] used the Penalized Augmented Lagrangian (PAL) method to accurately calculate the unyielded regions in the flow development of a Bingham plastic in a channel.

Studies of viscoelastic flow development are quite few; see [20,21] and references therein. An associated problem, which has been studied more in the viscoelastic community, is the contraction problem, where fluid flows from a wider pipe or channel into a narrower one, but the length required for re-establishment of fully developed flow is not often reported. Nevertheless, the results show that elasticity causes the flow to develop more slowly than the corresponding Newtonian one [21,22], or even compared to a generalised Newtonian one that exhibits the same degree of shear-thinning [23].

Shear-thinning or thickening is exhibited by a wide class of non-Newtonian fluids [24]. This is relatively easy to measure and to model, and, in some applications, it is the only non-Newtonian behaviour that needs to be accounted for in order to get a sufficiently accurate picture of the flow, despite the fluid possibly exhibiting also other kinds of non-Newtonian behaviour to some degree. Shear thinning is considered to be the predominant non-Newtonian characteristic of blood and other biofluids [4]. The decrease of viscosity with the shear rate is attributed to the destruction of rouleaux and the disaggregation of red blood cells which orient themselves in the direction of the flow [4].

Rheological models that account only for shear-thinning behaviour are the generalised Newtonian ones. The simplest non-Newtonian constitutive equation able to describe shear thinning is the power-law model, according to which the shear viscosity, η^*, is given by [24]

$$\eta^* = k^* \dot{\gamma}^{*n-1} \tag{1}$$

where k^* is the consistency index, n is the power-law exponent, and $\dot{\gamma}^*$ is the magnitude of the rate-of-strain tensor $\dot{\gamma}^*$, defined by $\dot{\gamma}^* = \sqrt{\dot{\gamma}^* : \dot{\gamma}^*/2}$. For $n = 1$, the viscosity is constant and the Newtonian model is recovered. The fluid is shear-thinning (pseudoplastic) when $n < 1$ and shear-thickening when $n > 1$.

The power-law model has been employed in most studies concerning entrance flows of shear-thinning fluids [1,16,25,26]. Fernandes et al. [2] employed Sisko's model, which is more general and reduces to the power-law model when the infinite shear-rate-viscosity is zero. In all these studies, the standard definition of the development length has been employed, assuming that the maximum velocity is a sufficient indicator of the flow development. Furthermore, in some of these studies an effort was made to collapse the development length curves as a function of the Reynolds number. While earlier works assumed this effort to be entirely successful, Poole and Ridley [1] showed that at low Reynolds numbers the collapsing of the curves is not perfect, but the development length still depends on the power-law exponent, similarly to what was mentioned above for viscoplastic flows. In particular, they found that, in the creeping flow limit, shear thinning causes the development length to increase due to the weakening of the viscous forces, up to a shear-thinning exponent of about $n = 0.4$; below this value, further strengthening of the shear-thinning behaviour causes a rapid reduction of the development length, as the fully developed velocity profile becomes more plug-like and similar to the inlet profile, as for the viscoplastic case. They also proposed a correlation between the development length, the Reynolds number, and the shear-thinning exponent n, that extends that of Durst et al. [6] for Newtonian pipe flow:

$$L_c = \left[\left(0.246n^2 - 0.675n + 1.03\right)^{1.6} + \left(0.0567 Re_{MR}\right)^{1.6} \right]^{1/1.6} \tag{2}$$

where the power-law index is in the range $0.4 < n < 1.5$ and Re_{MR} is the Reynolds number, as defined by Metzner and Reed [27],

$$Re_{MR} = \frac{\rho^* U^{*2-n} (2R^*)^n}{k^*} 8 \left(\frac{n}{2+6n}\right)^n = 8 \left(\frac{n}{1+3n}\right)^n Re \tag{3}$$

Here, ρ^* is the constant density of the fluid, U^* is the mean velocity in the pipe, R^* is the pipe radius, and

$$Re = \frac{\rho^* U^{*2-n} R^{*n}}{k^*} \tag{4}$$

is the standard definition of the Reynolds number.

More recently, Fernandes et al. [2] proposed the following correlation for channel flow development for $0 \leq Re_{MR} \leq 100$ and $1/3 \leq n \leq 1$:

$$L_c = \left[f^{1.6}(n) + (0.0444 Re_{MR})^{g(n)}\right]^{1/1.6} \tag{5}$$

where $Re = \rho^* U^{*2-n} H^{*n}/k^*$, H^* being the channel semi-width,

$$f(n) = 0.981 - \frac{0.355}{1 + 2e^{-(4.273n - 0.553)}} - e^{-(15.706n - 4.002)} \tag{6}$$

and

$$g(n) = -0.209n^2 + 0.645n + 1.225 \tag{7}$$

The Metzner-Reed Reynolds number in the case of channel flow, satisfies

$$Re_{MR} = 6\left(\frac{n}{1+2n}\right)^n Re \tag{8}$$

As noted in [2], with formula (5) the observed non-monotonic behaviour of L_c at lower Reynolds numbers is captured very well. Lee et al. [3] investigated numerically the developing flow of power-law fluids in pipes having superhydrophobic transverse grooves and showed that the corresponding development lengths are bigger than their counterparts for smooth pipes.

The behaviour of shear-thinning ($n < 1$) fluids is known to be in some respects similar to that of viscoplastic fluids. In both cases, the viscosity decreases with shear rate. In both pipe and channel flows, the stronger the shear-thinning is, the more flattened the fully developed velocity profile becoming similar to its viscoplastic counterpart. This indicates that monitoring the velocity field only at the centreline or midplane may be misleading, as in the viscoplastic case. Syrakos et al. [28] also argue that flows of shear-thinning power-law fluids cease in finite time, like their viscoplastic counterparts.

The objectives of the present work are: (a) to investigate whether the standard definition of the development length (L_c) provides an accurate criterion for the full development of the flow of power-law fluids in both pipes and channels; (b) to introduce an alternative definition of the development length, L_t, based on the evolution of the wall shear stress, and check its advantages and limitations. L_t is defined as the length needed for the wall shear stress to fall so that it deviates less than 1% from its fully-developed value. In fact, for many applications the wall shear stress is more crucial than the flow velocity – for example, blood vessels are lined with endothelial cells, whose growth, remodelling and function can be modified by the flow stresses [4]. Biological flows in the body commonly occur in tubular geometries, e.g., the flow of blood in vessels, or the flow of air in the lung airway tree. In medical and healthcare practice, flows of biological fluids can also occur in channels, e.g., the flow of blood in microfluidic diagnostic devices [29].

In Section 2, the equations governing the flow development of power-law fluids in pipes and channels are provided along with brief descriptions of the boundary conditions and the finite-element method employed for their solution. The numerical results, obtained for power-law exponents ranging between 0.2 and 1.5 and Reynolds numbers up to 1000 are presented and discussed in Section 3. Finally, the conclusions of this work are summarized in Section 4.

2. Governing equations and numerical method

Consider the isothermal flow of a power-law fluid entering a long cylindrical tube (or a channel) of radius R^* (or semi-width H^*) and length L^*_{mesh} with a uniform velocity U^*. Assuming that the flow is steady, incompressible and laminar, the continuity and momentum equations can be written as follows:

$$\nabla \cdot \mathbf{u}^* = 0 \tag{9}$$

and

$$\rho^* \mathbf{u}^* \cdot \nabla \mathbf{u}^* = -\nabla p^* + \nabla \cdot \tau^* \tag{10}$$

where p^* is the pressure field, $\mathbf{u}^*$ is the velocity vector, and τ^* is the viscous stress tensor. The constitutive equation of a power-law fluid is given by [24]:

$$\tau^* = \eta^*(\dot{\gamma}^*)\dot{\gamma}^* = k^* \dot{\gamma}^{*n-1} \dot{\gamma}^* \tag{11}$$

Substituting Eq. (11) into the momentum Eq. (10), one obtains a system of two partial differential equations for the velocity and pressure fields.

For convenience, the above governing equations are non-dimensionalized. As a length scale X^* we take the radius R^* in the case of a tube or the semi-width H^* in the case of a channel. The velocity vector is then scaled by the uniform velocity U^* (which is also the mean velocity), the components of $\dot{\gamma}^*$ by U^*/X^*, and the pressure and stress components by $k^* U^{*n}/X^{*n}$. With these scales, the dimensionless forms of Eqs. (9)–(11) become

$$\nabla \cdot \mathbf{u} = 0 \tag{12}$$

$$Re\, \mathbf{u} \cdot \nabla \mathbf{u} = -\nabla p + \nabla \cdot \tau \tag{13}$$

and

$$\tau = \dot{\gamma}^{n-1} \dot{\gamma} \tag{14}$$

The flow geometry and the boundary conditions for the cylindrical tube are illustrated in Fig. 1, where cylindrical coordinates (z, r) are used. The flow is assumed to be axisymmetric, i.e., two-dimensional: $\mathbf{u} = u(r,z)\mathbf{e}_z + v(r,z)\mathbf{e}_r$. At the inlet plane, the axial velocity is flat ($u = 1$) and the radial velocity is zero ($v = 0$). For a sufficiently long tube, the normal total stress component $-p + \tau_{zz}$ and the radial velocity also vanish at the outflow plane. The standard symmetry and no-slip/no-penetration conditions are applied at the axis of symmetry and the tube wall, respectively. The boundary conditions are quite similar in the case of a channel, where cartesian coordinates (x, y) are employed.

Standard finite elements are employed in order to numerically solve the system of Eqs. (12) and (13) for the velocity and pressure fields, which are approximated using biquadratic and bilinear basis functions, respectively [8]. The non-linear system of the discretized equations was solved using Newton's method with a convergence tolerance equal to 10^{-4}. The power-law constitutive equation implies infinite ($n < 1$) or zero ($n > 1$) viscosity at zero rate of deformation. To avoid numerical difficulties, solutions were obtained by starting from the Newtonian solution and using continuation on n.

3. Numerical results

We have carried out numerical simulations of the flow development of power-law fluids in both pipes and channels for power-law exponents ranging from 0.2 to 1.5 and for Reynolds numbers from zero up to 1000. Note that with the ideal power-law constitutive model employed here, the viscosity is allowed to go to infinity. For the development flows considered in this work, the only place that this would theoretically occur is at the centreline/plane of symmetry once the flow has become fully developed. However, there are no Gauss points located exactly on this boundary, and furthermore the grid cells there are coarser compared to those near the wall, so that the viscosity is not calculated at any point where it would, even theoretically, be infinite. On the other hand, the high values of viscosity and the associated stiffness do create numerical difficulties at low values of the power-law exponent, and hence we were unable to attain solutions for $n < 0.22$ for $Re = 0$ and for $n < 0.3$ for $Re > 0$, despite the use of continuation. The convergence of the numerical results has been confirmed using meshes of different refinement and different lengths. All the results presented below have been obtained with a rather long mesh with $L_{\text{mesh}} = 1120$, which was found to be adequately long for the highest value of the Reynolds number consid-

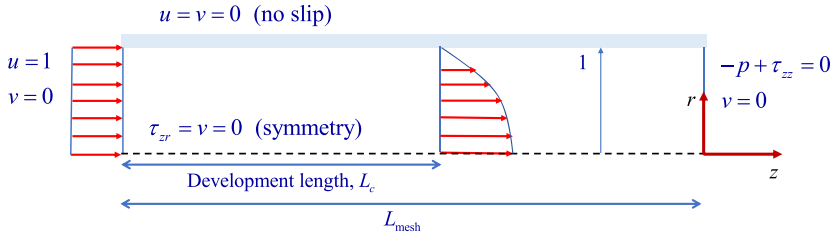

Fig. 1. Geometry and dimensionless boundary conditions for the flow development in a cylindrical tube.

ered here. The distribution of the development length across the pipe, $L(r)$, has been calculated by determining the distance beyond which the velocity for a given value of r lied between 0.99–1.01 times its fully developed value. Thus, the standard centreline development length is simply $L_c = L(0)$ and the global development length is $L_g = \max_{0\le r\le 1} L(0)$. We have also calculated the wall shear stress development length, L_t, which is defined in a similar manner. To facilitate comparisons with the literature, the development lengths are scaled by $2X^*$, i.e., by the diameter of the tube or the width of a channel. However, all other length quantities are scaled by X^*. It should also be noted that the Reynolds number, defined by Eq. (4), is also expressed in terms of X^*.

3.1. Pipe flow development

The development of the axial velocity in the case of a pipe for $Re = 0$ and different values of the power-law exponent, $n = 1.5, 1, 0.5$ and 0.22, is illustrated in Fig. 2, where velocity distributions at different distances

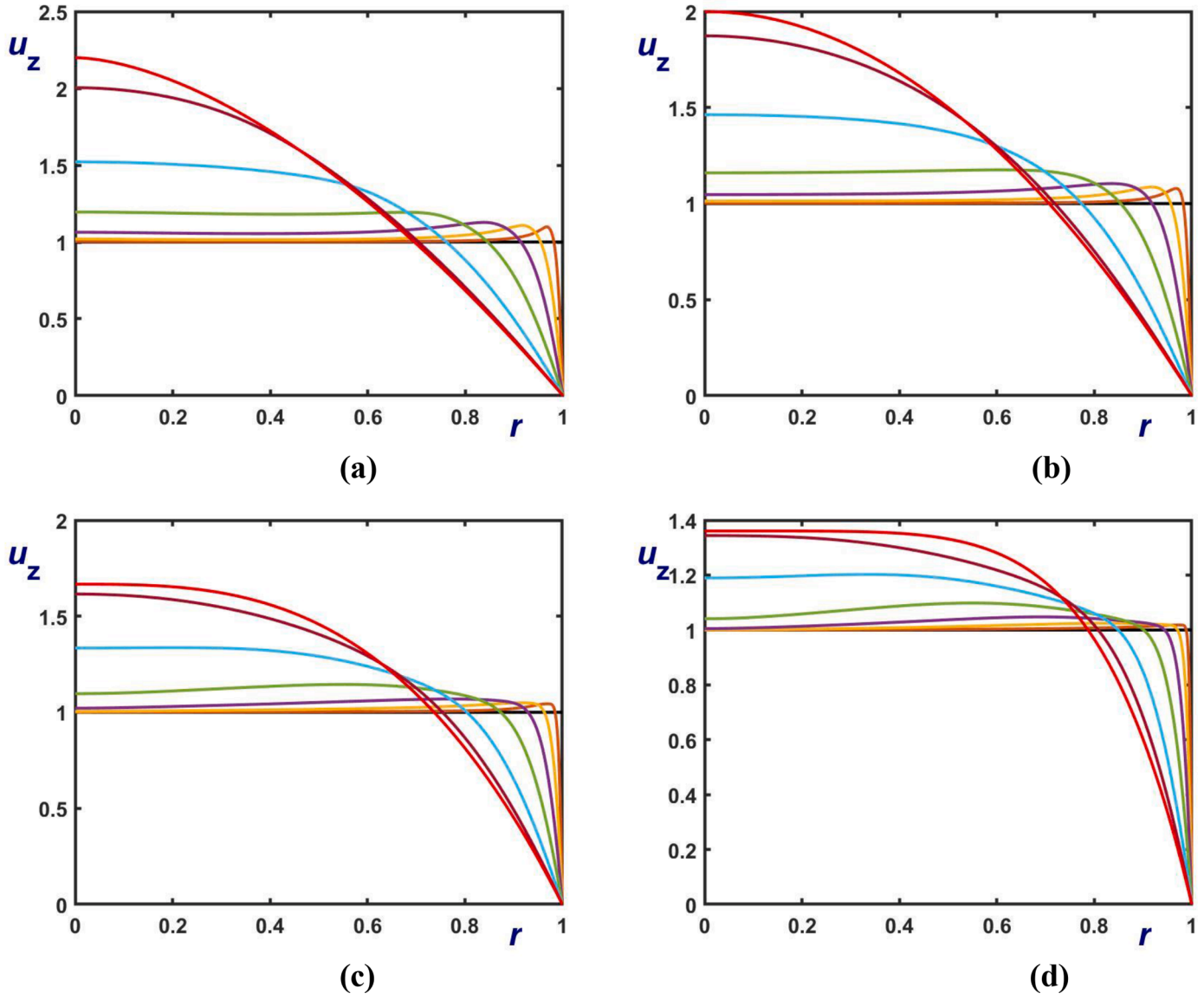

Fig. 2. Velocity profiles at $z = 0, 0.02, 0.052, 0.1, 0.2, 0.40, 0.81$ and 20 in pipe flow development when $Re = 0$ for different values of the power-law exponent: (a) $n = 1.5$; (b) $n = 1$; (c) $n = 0.5$; (d) $n = 0.22$. It should be noted that the scales of the vertical axis are different.

from the inlet are plotted. The initial overshoots of the velocity distributions near the wall are characteristic of the flow; the fluid particles in a layer adjacent to the wall decelerate due to the no-slip boundary condition at the wall and, thus, particles in the neighbouring layers need to accelerate for the mass to be conserved. The velocity distributions eventually tend to the corresponding Poiseuille flow solution, which is given by [24]:

$$u = \frac{(2+\alpha)n+1}{n+1}\left(1 - r^{1/n+1}\right) \tag{15}$$

where α is an auxiliary parameter taking the values 1 and 0 for a pipe and a channel, respectively; obviously, r should be replaced by y for channel flow in the x direction. The velocity profile becomes more flattened as the power-law exponent is reduced, and, hence, the fully-developed maximum velocity,

$$u_{c\infty} = u(0) = \frac{(2+\alpha)n+1}{n+1} \tag{16}$$

decreases from 3 ($n \to \infty$; shear-thickening limit) to unity ($n \to 0$; shear-thinning limit), attaining the value of 2 when the fluid is Newtonian ($n = 1$). It is clear, e.g., by comparing the velocity distributions at $z = 0.81$ and $z = 20$, that the distance required for the centreline velocity to re-adjust to its Poiseuille-flow value is reduced as the fluid becomes more shear thinning (fluid particles at the symmetry axis have to travel a shorter distance in order to accelerate up to the fully-developed maximum velocity). However, the development of the axial velocity near the wall becomes slower, as can be observed in Fig. 2d where $n = 0.22$, despite the fact that the velocity overshoots are less pronounced.

The effect of the power-law exponent on the distribution of the development length $L(r)$ in a pipe is illustrated in Fig. 3, where the results for $n = 1.5$, 1 and 0.22 are shown. One observes that for the first two values of n, i.e., for shear-thickening and Newtonian fluids, the flow develops more slowly along the axis of symmetry and thus the global and centreline development lengths coincide, $L_c = L_g$. It is clear that $L(r)$ decreases initially to pass through a sharp minimum within the tube before starting increasing again towards the wall. This minimum obviously corresponds to the radial distance where the fully-developed velocity is equal to the mean velocity. The development length is not zero, since fluid particles may decelerate initially and then accelerate (or vice versa) to attain again their initial velocity. Nevertheless, with shear-thinning fluids ($n < 1$) the flow within the pipe develops more slowly. Below a critical value of the exponent in the shear-thinning regime, however, $L(r)$ exhibits a local maximum within the pipe and its global maximum at the wall, in which case $L_c < L_g$.

Fig. 4 shows the development of the centreline velocity and the wall shear stress for the Newtonian flow ($n = 1$) at zero Reynolds number. The centreline velocity (Fig. 4a), which is unity at the inlet, increases exhibiting a small, hard to see, overshoot to reach asymptotically the value $u_{c\infty}$, as given by Eq. (16). On the other hand, the wall shear stress (Fig. 4b), becomes infinite at the inlet due to the sudden change of the velocity boundary condition from unity to zero. The rapid deceleration at the wall is associated with high wall shear stresses that gradually decrease to their Poiseuille value, while the acceleration at the core requires pressure gradients that are larger in magnitude than the eventual Poiseuille value. After exhibiting a slight, almost not discernible, undershoot, the wall shear stress converges asymptotically to its fully developed value:

$$\tau_{w\infty} = \left(2 + \alpha + \frac{1}{n}\right)^n \tag{17}$$

($\tau_{w\infty} = 4$ in the case of Newtonian flow in a pipe).

The effect of the Reynolds number is illustrated in Fig. 5, where the three development lengths for $n = 1.5$, 1 and 0.5 are plotted versus the Reynolds number. Recall that unlike other studies in the literature (e.g.,

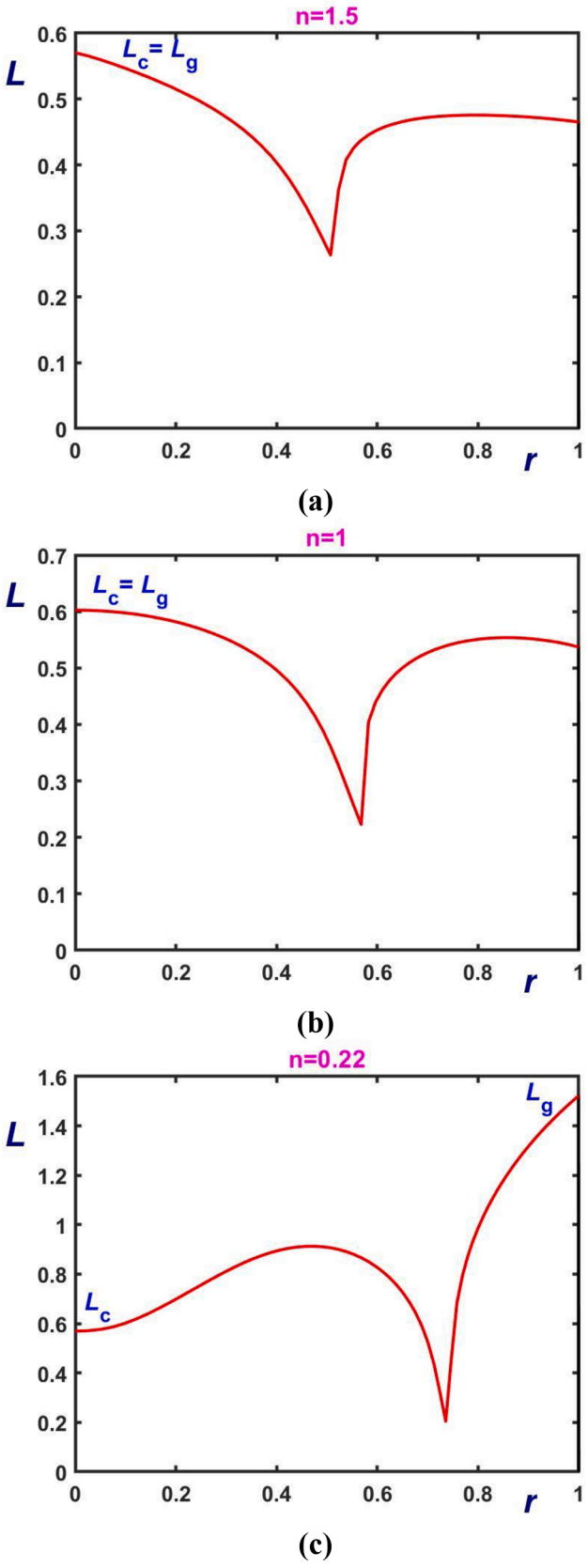

Fig. 3. Development length in pipe flow for $Re = 0$ as a function of the radius: (a) $n = 1.5$ (shear thickening); (b) $n = 1$ (Newtonian); (c) $n = 0.22$ (shear thinning).

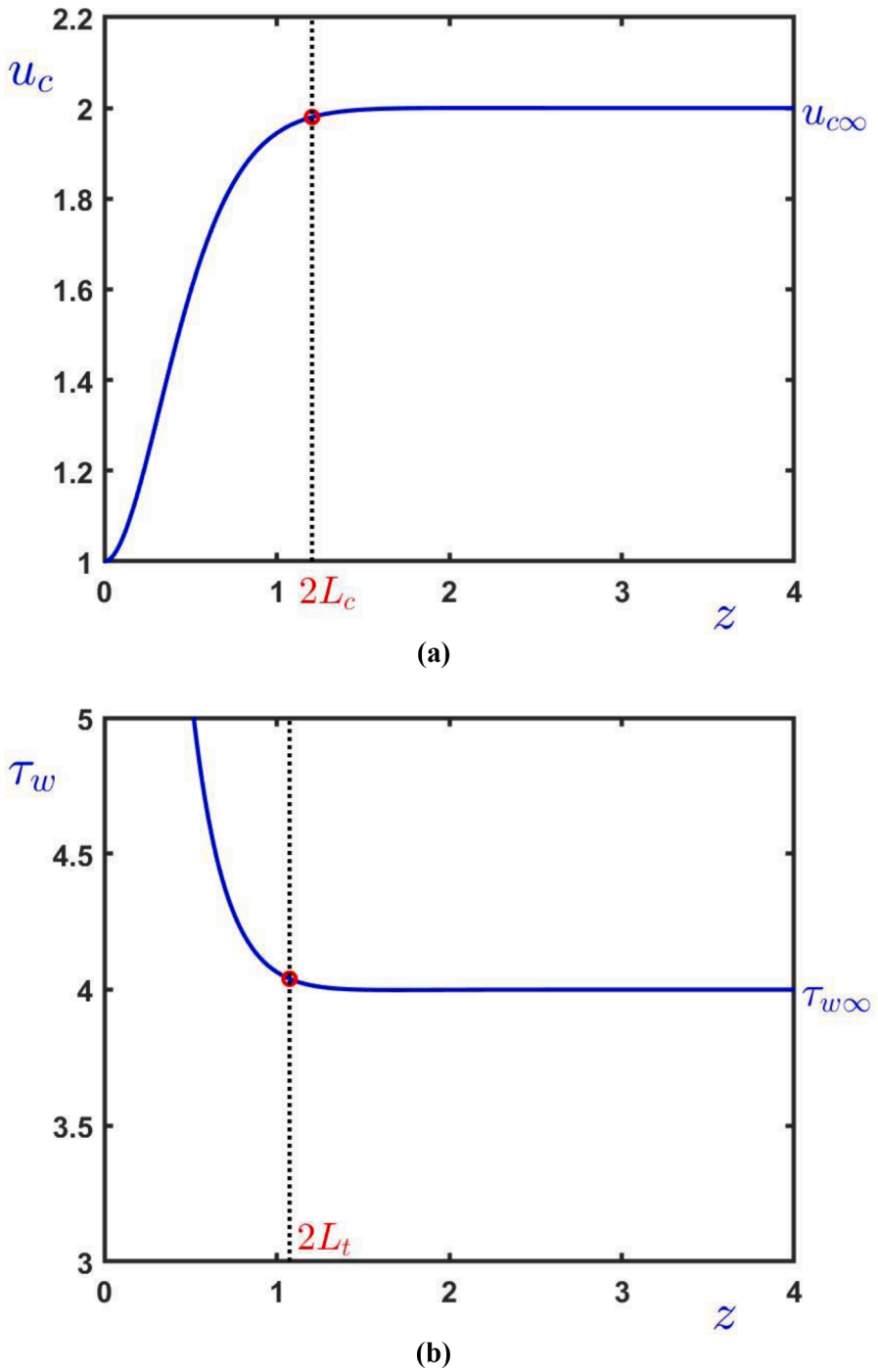

Fig. 4. Newtonian ($n = 1$) flow development in a pipe when $Re = 0$: (a) Development of the centreline velocity; (b) Development of the wall shear stress.

[6]), the Reynolds number is defined not in terms of the diameter, but in terms of the pipe radius. In a logarithmic plot, all three development lengths initially exhibit a plateau and then start increasing more rapidly with the Reynolds number. The centreline development length practically coincides with the global development length only when $n \geq 1$. In the shear thinning regime, L_c is lower than L_g, and the differences are more pronounced at lower Reynolds numbers. In Newtonian flow ($n = 1$, Fig. 5b), centreline and global development lengths coincide while the stress development length is smaller, especially at low values of the Reynolds number. The difference of L_t from the other development lengths is reduced as Re is increased and the three curves eventually merge for $Re > 20$. The situation changes with shear thinning fluids. When $n = 0.5$, the difference between L_c and L_g is more pronounced at low values of the Reynolds number ($Re < 10$) and decreases as the latter number is increased. With the exception of the interesting jump exhibited at low Reynolds numbers when the power-law exponent is high (Fig. 5a), the stress development length is smaller than L_c and L_g. The differences are less visible when both the power-law exponent and the Reynolds number are increased. For $n \geq 1$, the three development lengths essentially merge for $Re > 20$. For $n < 1$, no merging is observed at high Re; at low Re, L_t is closer to L_c. Of course, if the Metzner-Reed definition of the Reynolds number is used instead the three curves collapse at high Reynolds numbers.

In the case when $n = 1.5$ (Fig. 5a), L_t appears to be higher than L_c and L_g for small Reynolds numbers exhibiting a sudden jump at $Re \approx 2.5$, becoming smaller than the centreline development length and then

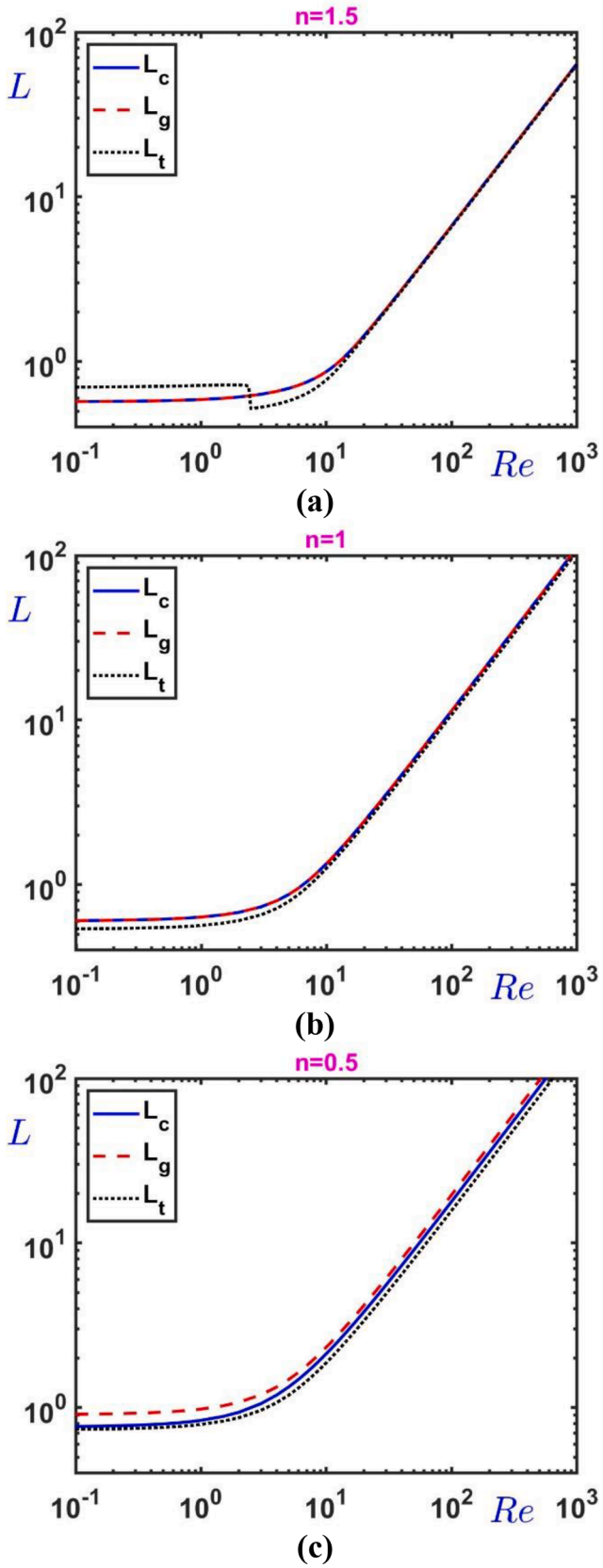

Fig. 5. The three development lengths in flow development of power-law fluids in a pipe: (a) $n = 1.5$; (b) $n = 1$; (c) $n = 0.5$.

starts to increase, converging to L_c, as the Reynolds number is increased. This peculiar behaviour is a consequence of the stress undershoot that occurs before the flow is fully developed and the definition of L_t. As illustrated in Fig. 6, the stress undershoot is relatively big at low Reynolds numbers and the observed stress minimum is less than $0.99\tau_{w\infty}$. Therefore, the flow becomes formally fully developed downstream of the stress minimum. Above a certain critical value of the Reynolds number, the stress minimum eventually becomes greater than $0.99\tau_{w\infty}$. In such a case, the flow is formally fully-developed upstream of the stress minimum, when the stress reaches the value of $1.01\tau_{w\infty}$, and this explains the sudden jump in the value of the stress development length. Similar explanations, based on velocity overshoots or undershoots, can be provided for the sudden jumps exhibited, in certain cases, by the global development length in the case of channel flow, which is discussed below.

In Fig. 7, the development lengths are plotted versus the power-law exponent for $Re = 0$, 10 and 100. We observe that L_g and L_c essentially coincide for $n > 0.7$, which implies that the flow readjustment is indeed slower at the centreline. Below this value, L_g is higher than L_c. This is somehow expected since the velocity profile becomes more flattened as the power-law exponent is reduced. The difference between these two lengths becomes more pronounced at lower values of n and Re, which implies that the flow is not fully developed at a distance equal to the standard development length. While L_g is a decreasing function of the power-law exponent, the behaviour of L_c is non-monotonic. The standard development length L_c appears to initially increase with the power-law exponent, exhibiting a maximum after which it decreases merging eventually with L_g. The calculated values of L_c agree well with those of Poole and Ridley [1]. The stress development length appears to be smaller than the other two lengths at moderate and high Reynolds numbers and the differences become bigger as the power-law exponent is reduced. At low values of the Reynolds numbers, however, L_t becomes bigger than L_c in the regime where the latter is an increasing function of the power-law exponent (Fig. 7a). The sudden jump of the stress development length in Fig. 7a for $n \approx 1.45$ is obviously due to the stress overshoot effect discussed above.

The effect of the power-law exponent on the three development lengths is illustrated in Fig. 8, where results for $n = 0.5$, 1, and 1.5 are shown. As the power-law exponent is increased the corresponding curves are shifted upwards retaining in general their shape, the only exception being the left branch of the stress-development-length curve for $n = 1.5$ (before the sudden jump). The results of Fig. 8a show that the power-law exponent affects the value of the centreline development length not only at high but also at low Re, as was pointed out by Poole and Ridley (2007).

As a test to the present calculations, the results for the centreline development length for $n = 1.5$, 1 and 0.5 are compared with the predictions of the empirical formula (2) proposed in [1]. As illustrated in Fig. 9, Eq. (2) describes quite well the variation of the centreline development length with the Reynolds number and the power-law index. For $n = 1.5$, some minor discrepancies are observed for intermediate Re, whereas for $n = 0.5$ some differences are observed at low and high values of the Re. According to Poole and Ridley [1], the agreement of Eq. (2) to the data was better than 5% except at the highest Reynolds numbers, especially for $n = 0.4$ and 1.5.

3.2. Channel flow development

The numerical results for the flow development in a channel differ from their pipe-flow counterparts in that the centreline development length does not coincide with the global development length in creeping ($Re = 0$) Newtonian flow. L_c and L_g become practically the same only above a critical value of the power-law exponent in the shear-thickening regime ($n > 1$). This can be seen in Fig. 10, where the distributions of $L(r)$ for $Re = 0$ and three different values of the power-law exponent

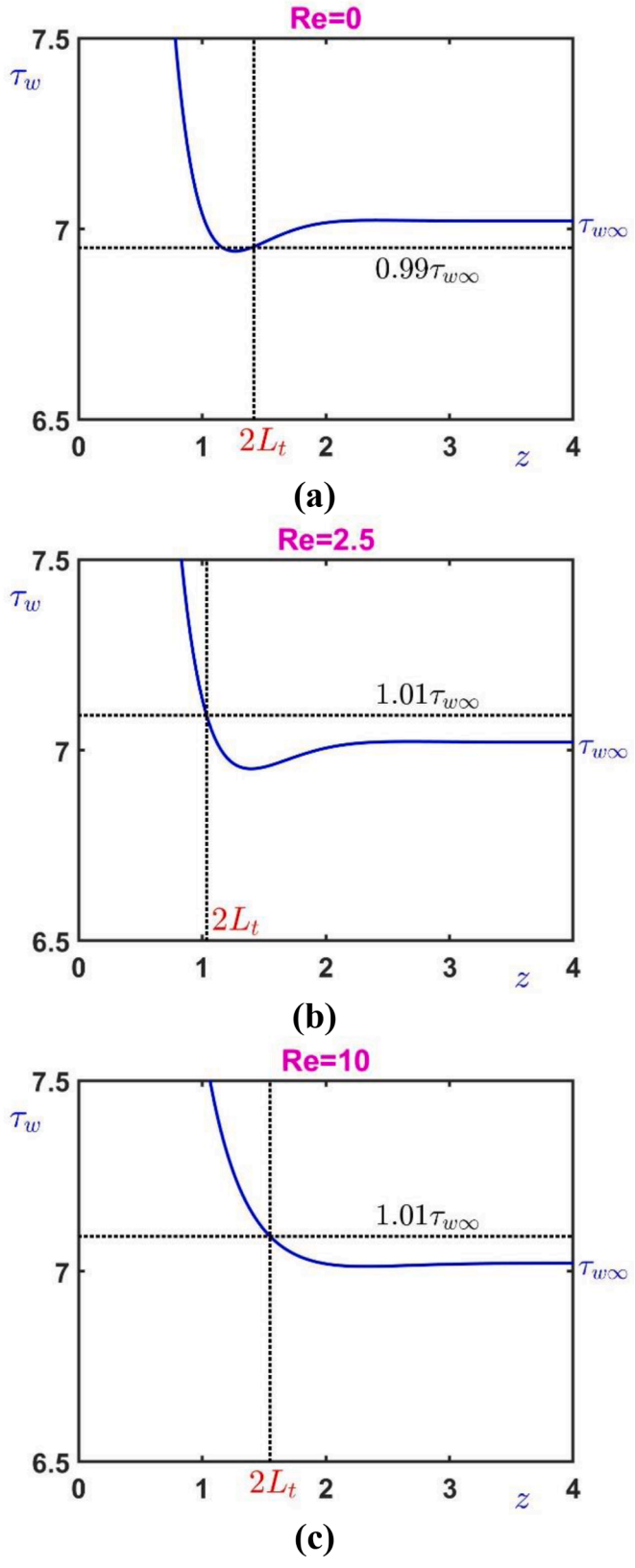

Fig. 6. Distribution of the wall shear stress when $n = 1.5$: (a) $Re = 0$; (b) $Re = 2.5$; (c) $Re = 10$. When $Re < 2.5$ the point where the flow becomes fully developed is downstream of the stress minimum. When $Re = 2.5$ the minimum is not so sharp and the flow is assumed to become fully-developed upstream of the stress minimum, which explains the sudden fall of L_t. At even higher values of the Reynolds number, the wall shear stress distribution decreases monotonically. Axisymmetric flow.

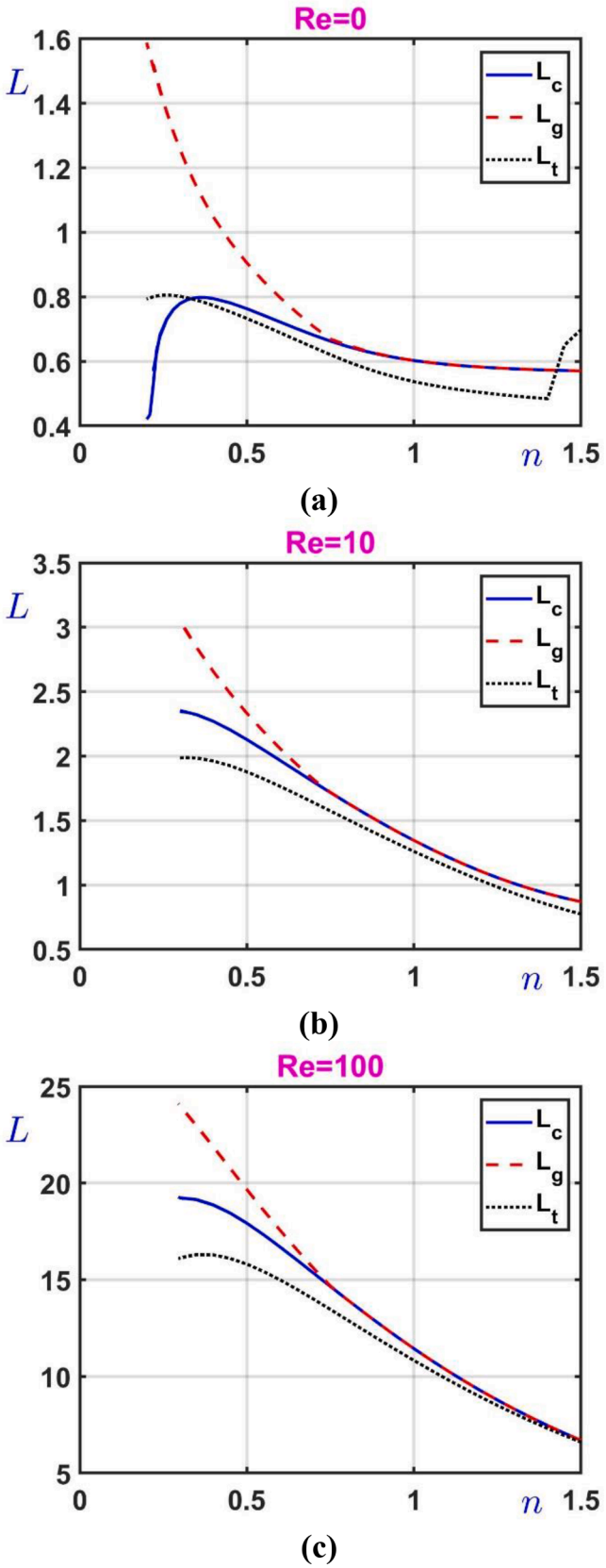

Fig. 7. Centreline, global, and stress development lengths for the flow development of power-law fluids in pipes: (a) $Re = 0$; (b) $Re = 10$; (c) $Re = 100$.

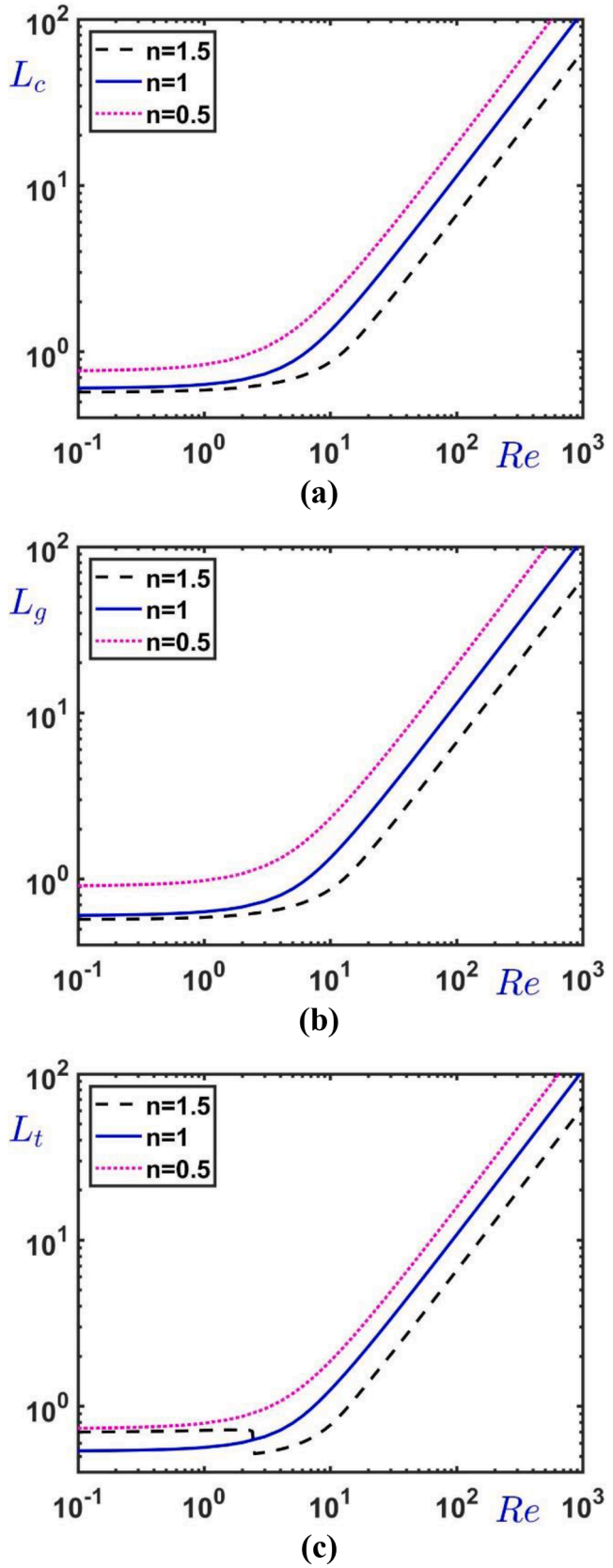

Fig. 8. Effect of the power-law exponent in pipe flow development on: (a) centreline development length, L_c; (b) Global development length, L_g; (c) Stress development length, L_t.

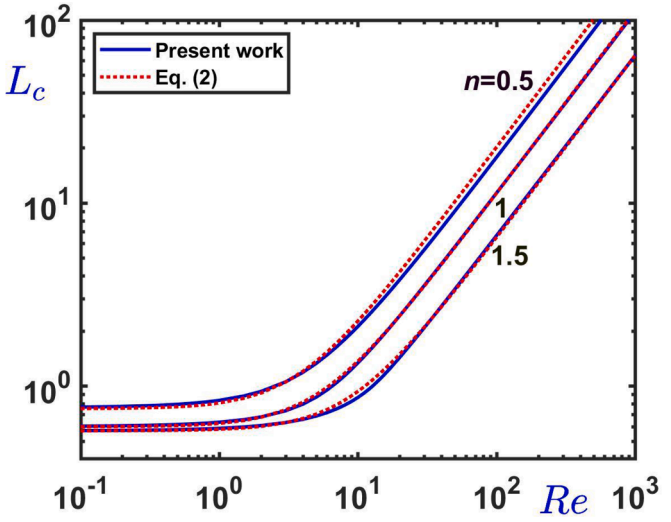

Fig. 9. Comparisons of the calculated centreline development lengths for $n = 0.5$, 1 and 1.5 with the predictions of the empirical formula (2) of Poole and Ridley (2007) for pipe flow development.

($n = 1.5$, 1, and 0.4) are shown. The sudden jump of $L(r)$ near the wall when $n = 1.5$ is obviously due to an undershoot of the velocity similar to that of the wall shear stress in Fig. 4. Ignoring this jump, we observe that $L_c = L_g$ only in the shear-thickening regime. Another difference from Newtonian pipe flow ($n = 1$, Fig. 3b) is that the maximum of $L(r)$ occurs in the interior of the channel (Fig. 10b). The behaviour of $L(r)$ for lower values of n in the two geometries is quite similar.

The effect of the Reynolds number for $n = 1.5$, 1, and 0.5 is illustrated in Fig. 11. Clearly, L_c is smaller than L_t and L_g in all cases. For lower values of the power-law exponent the observed differences become more pronounced which implies that using the classical definition of the development length is not reliable in the channel geometry. As already mentioned, the result that the flow develops more slowly at the wall has also been suggested by the numerical simulations of Kountouriotis et al. [8] for Newtonian flow in the presence of wall slip, where the wall development length was defined in terms of the slip velocity. Since the latter is an increasing function of the wall shear stress, the wall development length is equivalent to the stress development length considered here provided that finite wall slip occurs. For values of Reynolds number above $Re = 10$, L_t is bigger than L_g in the shear-thickening regime, roughly equal to L_g for values of the power-law exponent near unity (Newtonian fluid) and smaller than L_g in the shear thinning regime. When $n = 1.5$, sudden jumps are observed for L_t and L_g, due to undershoots of the wall shear stress and overshoots of the velocity. L_t and L_g are much bigger than L_c at low Re. For low Reynolds numbers, the three development lengths essentially coincide for power-law exponents around unity (Fig. 11b). As the fluid becomes more shear thinning, the differences between the three development lengths become more important for low Reynolds numbers.

In Fig. 12, the variation of the development lengths with the power-law exponent is illustrated for $Re = 0$, 10 and 100. Note the non-monotonicity of L_c at zero Reynolds number, also observed in pipe flow. This curve agrees well with the results of Fernandes et al. [2]. Jumps of the stress and global development length are observed in the shear-thickening regime only when the Reynolds number is low (Fig. 12a). The stress development length lies between L_c and L_g for values of n in the shear-thinning regime. The centreline and global development lengths tend to merge as n is increased. This merging is delayed at higher Reynolds numbers. When $Re = 10$ (Fig. 12b), L_t becomes smaller than the velocity-based development lengths for $n > 1.35$. When $Re = 100$, however, L_t, exceeds L_g for $n > 1$, i.e., in the shear-thickening regime.

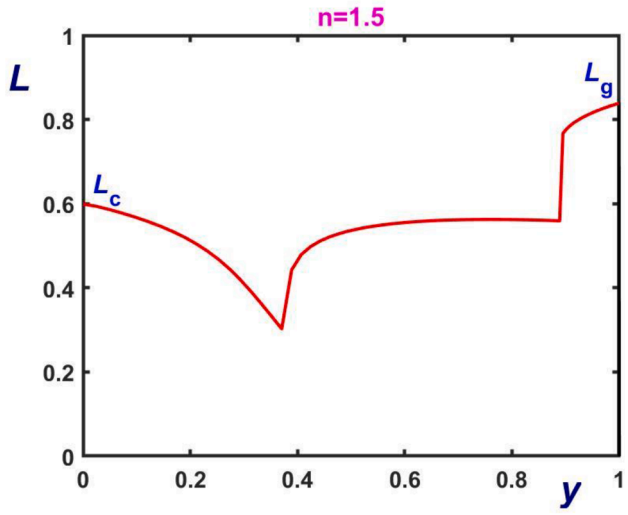

(a)

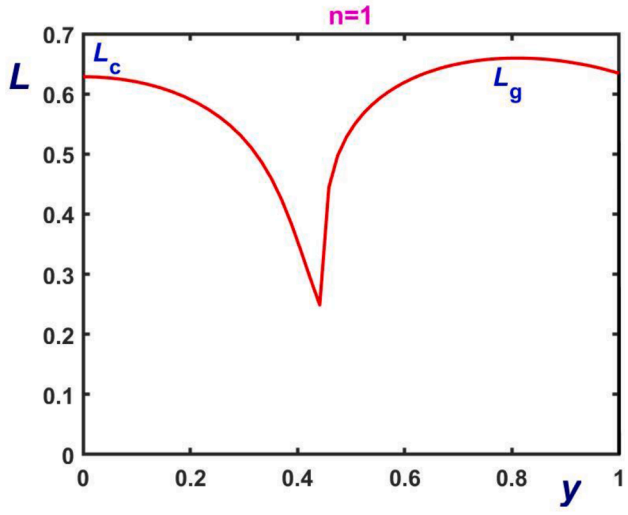

(b)

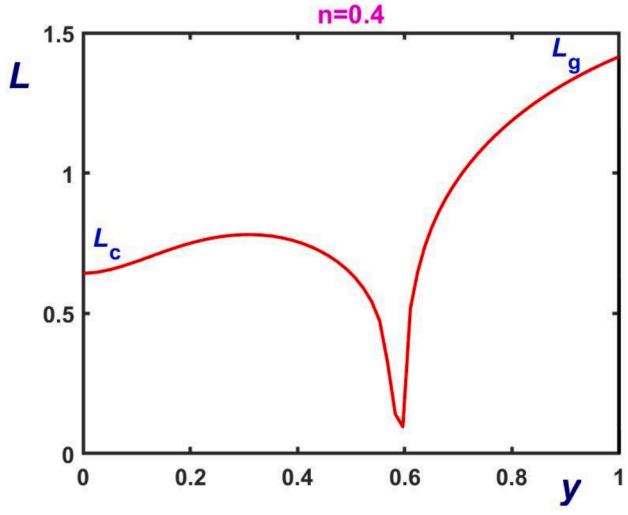

(c)

Fig. 10. Development length in channel flow for $Re = 0$ as a function of the distance from the midplane: (a) $n = 1.5$ (shear thickening); (b) $n = 1$ (Newtonian); (c) $n = 0.4$ (shear thinning).

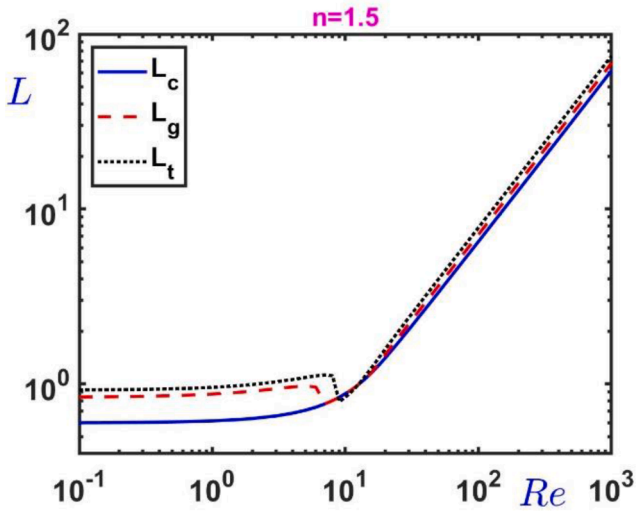

(a)

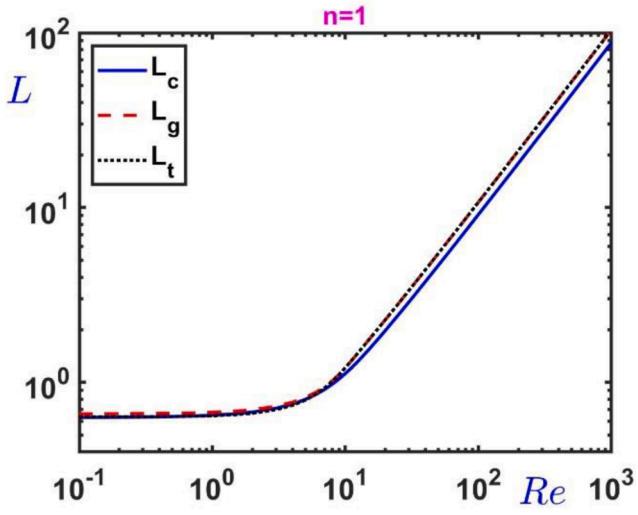

(b)

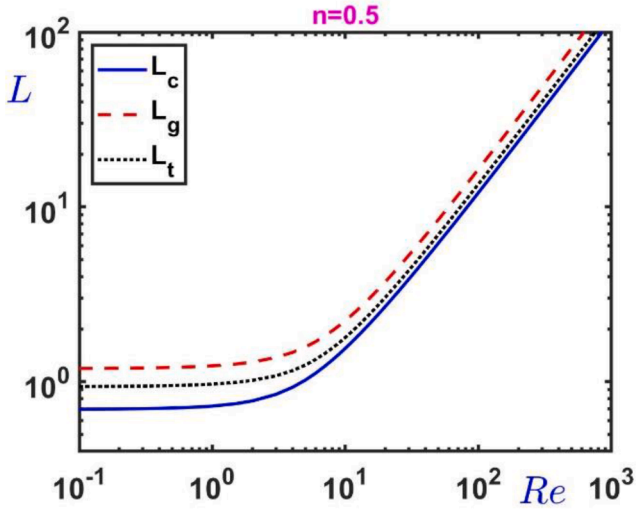

(c)

Fig. 11. The three development lengths in flow development of power-law fluids in a channel: (a) $n = 1.5$; (b) $n = 1$; (c) $n = 0.5$.

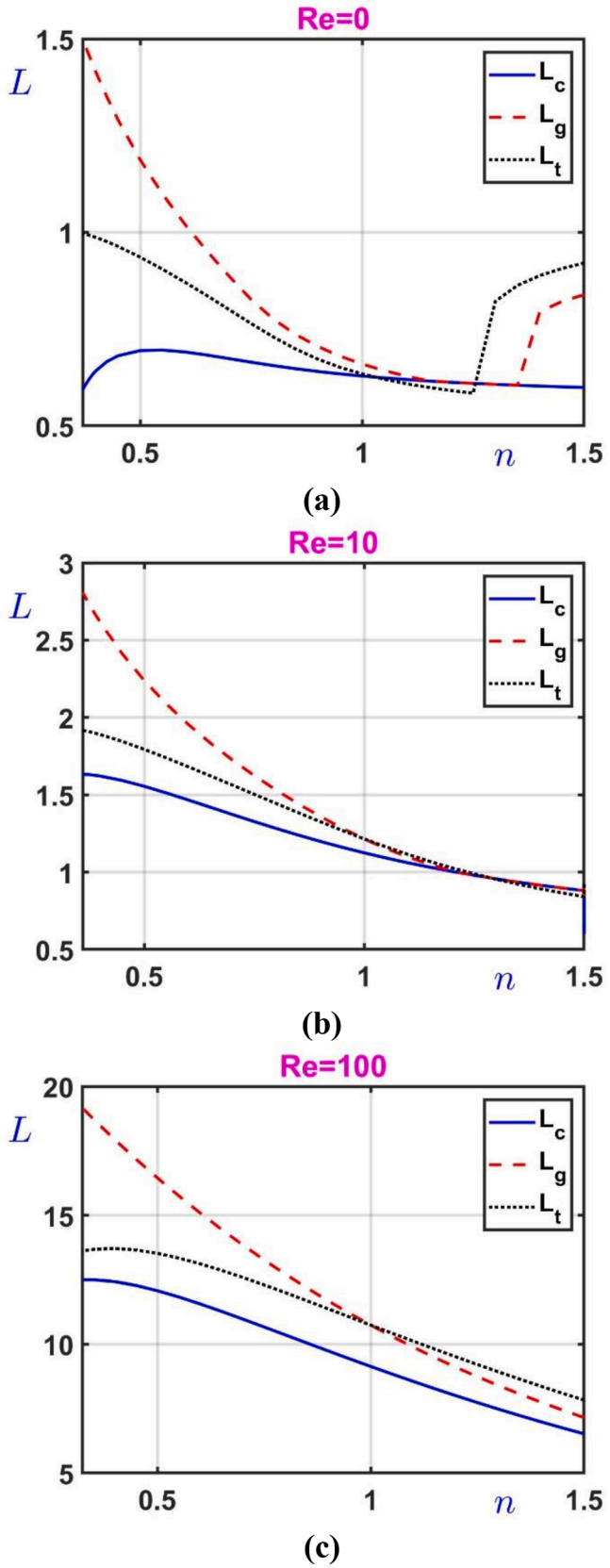

Fig. 12. Centreline, global, and stress development lengths for the flow development of power-law fluids in channels: (a) $Re = 0$; (b) $Re = 10$; (c) $Re = 100$.

Finally, comparisons have been made with the predictions of the empirical correlation (5), proposed by Fernandez et al. [2] for $0 \leq Re_{MR} \leq 100$ and $1/3 \leq n \leq 1$, i.e., only for shear-thinning power-law fluids. As shown in Fig. 13, where the numerical results for $n = 0.5$, 1, and 1.5 and $Re \leq 1000$ are plotted, there is a very good agreement with the empirical correlation even for the shear-thickening case. Bigger differences are observed for the shear thinning fluid ($n = 0.5$) when $Re > 10$.

4. Conclusions

In this numerical study, we have investigated the flow development of power-law fluids in pipes and channels. In addition to the standard definition of the development length, L_c, which is based on the centreline velocity, we also considered the global development length, L_g, defined over the axial velocity distribution, and the stress development length, L_t, based on the development of the wall shear stress. Results have been obtained for $0.2 \leq n \leq 1.5$ and $0 \leq Re \leq 1000$.

The results for pipe flow development showed that the standard development length L_c is a reliable indicator of flow development only for values of the power-law exponent greater than 0.7, independently of the Reynolds number. For more shear-thinning fluids ($n < 0.7$), however, the centreline development length is misleading, since the flow develops more slowly far from the axis of symmetry. The relative differences are more striking at low Reynolds numbers at which L_g can be four times L_c. Hence, attention must be paid when using the assumption of fully developed flow for shear thinning fluids in pipes when the Reynolds number is low, e.g., for flows of blood or other biofluids in small vessels. The wall stress development length in a cylindrical tube is always shorter than the centreline development length, except at low values of the Reynolds number and the power-law exponent ($n < 0.4$).

In contrast to its pipe-flow counterpart, the standard development length is not a reliable criterion for channel flow development. This coincides with the global development length only for low Reynolds numbers and for certain values of the power-law exponent in the shear thickening regime ($n > 1$). The difference between L_g and L_c increases with inertia and shear thinning. Another interesting finding is that the stress development length is also greater than the standard development length. As already mentioned, L_t is also greater than the global development length in the shear thickening regime, when the Reynolds number is high. Thus, the use of the stress development length makes more sense in channel flows, where flow development is slower near the

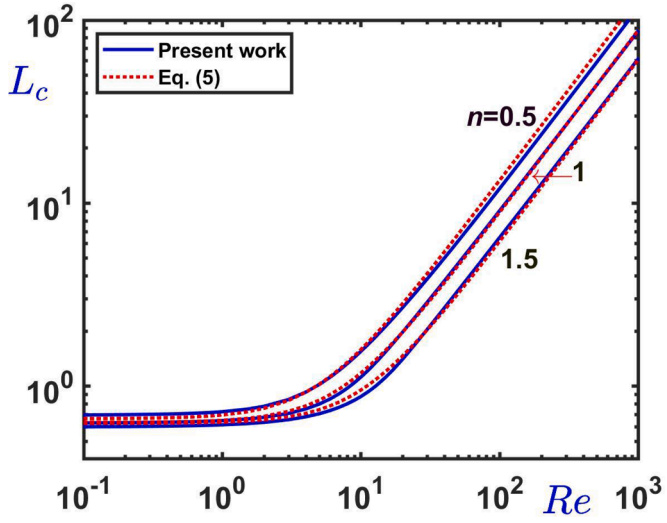

Fig. 13. Comparisons of the calculated centreline development lengths for $n = 0.5$, 1 and 1.5 with the predictions of the empirical formula (5) of Fernandez et al. [2] for channel flow development.

wall. This was also deduced by Kountouriotis et al. [8], who studied the development of Newtonian flow in channels and pipes in the presence of wall slip and reported that, in contrast to pipe flow, in channels the slip-velocity development length is bigger than the standard development length. The slip development length is equivalent to the stress development length defined in the present work, which, however, is more general, since it also applies in the absence of wall slip.

Declaration of Competing Interest

The authors declare that they have no known competing financial interests or personal relationships that could have appeared to influence the work reported in this paper.

Data availability

No data was used for the research described in the article.

References

[1] R.J. Poole, S.B. Ridley, Development length requirements for fully-developed laminar pipe flow of inelastic non-Newtonian liquids, ASME J. Fluids Eng. 129 (2007) 1281–1287.
[2] C. Fernandes, L.L. Ferrás, M.S. Araujo, J.M. Nóbrega, Development length in planar channel flows of inelastic non-Newtonian fluids, J. Non-Newtonian Fluid Mech. 255 (2018) 13–18.
[3] M.W. Lee, K.H. Yu, Y.H. Teoh, H.W. Lee, M.A. Ismail, Developing flow of power-law fluids in circular tube having superhydrophobic transverse grooves, J. Adv. Res. Fluid Mech. Thermal Sci. 56 (2019) 1–9.
[4] J.B. Grotberg, Biofluid Mechanics: Analysis and Applications, Cambridge University Press, Cambridge, 2021.
[5] A.R. Clark, M. Lin, M. Tawhai, P. Saghian, J.L. James, Multiscale modelling of the feto–placental vasculature, Interface Focus 5 (2015), 20140078.
[6] F. Durst, S. Ray, B. Unsal, O.A. Bayoumi, The development lengths of laminar pipe and channel flows, ASME J. Fluids Eng. 127 (2005) 1154–1160.
[7] A.K. Mohanty, S.B.L. Asthana, Laminar flow in the entrance region of a smooth pipe, J. Fluid Mech. 90 (1978) 433–447.
[8] Z. Kountouriotis, M. Philippou, G.C. Georgiou, Development lengths in Newtonian Poiseuille flows with wall slip, Appl. Math. Comp. 291 (2016) 98–114.
[9] P. Panaseti, K.D. Housiadas, G.C. Georgiou, Newtonian Poiseuille flows with pressure-dependent slip, J. Rheol. 57 (2013) 315–332.
[10] Y. Joshi, B.R. Vinoth, Entry lengths of laminar pipe and channel flows, ASME J. Fluids Eng. 140 (6) (2018), 061202.
[11] M. Philippou, Z. Kountouriotis, G.C. Georgiou, Viscoplastic flow development in tubes and channels with wall slip, J. Non-Newtonian Fluid Mech. 234 (2016) 69–81.
[12] G. Vlastos, D. Lerche, B. Koch, The superposition of steady on oscillatory shear and its effect on the viscoelasticity of human blood and a blood-like model fluid, Biorheology 34 (1997) 19–36.
[13] M. Armstrong, J. Horner, M. Clark, M. Deegan, T. Hill, C. Keith, L. Mooradian, Evaluating rheological models for human blood using steady state, transient, and oscillatory shear predictions, Rheol. Acta 57 (2018) 705–728.
[14] S.S. Shibeshi, W.E. Collins, The rheology of blood flow in a branched arterial system, Appl. Rheol. 15 (2005) 398–405.
[15] G.C. Vradis, J. Dougher, S. Kumar, Entrance pipe flow and heat transfer for a Bingham plastic, Int. J. Heat Mass Transfer 36 (1993), 543-522.
[16] S. Ookawara, K. Ogawa, N. Dombrowski, E. Amooie-Foumeny, A. Riza, Unified entry length correlation for Newtonian, power law and Bingham fluids in laminar pipe flow at low Reynolds number, J. Chem. Eng. Japan 33 (2000) 675–678.
[17] R.J. Poole, R.P. Chhabra, Development length requirements for fully developed laminar pipe flow of yield stress fluids, ASME J. Fluids Eng. 132 (2010), 034501.
[18] P. Panaseti, G.C. Georgiou, Viscoplastic flow development in a channel with slip along one wall, J. Non-Newtonian Fluid Mech. 248 (2017) 8–22.
[19] Y. Dimakopoulos, G. Makrigiorgos, G.C. Georgiou, J. Tsamopoulos, The PAL (Penalized Augmented Lagrangian) method for computing viscoplastic flows: a new fast converging scheme, J. Non-Newtonian Fluid Mech. 236 (2018) 23–51.
[20] K. Yapici, Y. Karasozen, Y. Uludag, Numerical analysis of viscoelastic fluids in steady pressure-driven channel flow, ASME J. Fluids Eng. 134 (2012), 051206.
[21] J. Bertoco, R.T. Leiva, L.L. Ferrás, A.M. Afonso, A. Castelo, Development length of fluids modelled by the gPTT constitutive differential equation, Appl. Sci. 11 (2021) 10352.
[22] X.-.W. Li, G.-.B. Wen, D. Li, Computer simulation of non-Newtonian flow and mass transport through coronary arterial stenosis, Appl. Maths. Mech. 22 (2001) 409–424.
[23] A. Syrakos, Y. Dimakopoulos, J. Tsamopoulos, Theoretical study of the flow in a fluid damper containing high viscosity silicone oil: effects of shear-thinning and viscoelasticity, Phys. Fluids 30 (2018), 030708.
[24] R.B. Bird, C.F. Curtiss, R.C. Armstrong, O. Hassager, Dynamics of Polymeric Liquids, Vol. 1, Fluid Mechanics, 2nd edn, Wiley, New York, 1987.
[25] R.C. Gupta, On developing laminar non-Newtonian flow in pipes and channels, Nonlin. Anal. Real World Appl. 2 (2001) 171–193.
[26] R. Chebbi, Laminar flow of power-law fluids in the entrance region of a pipe, Chem. Eng. Sci. 57 (2002) 4435–4443.
[27] A.B. Metzner, J.C. Reed, Flow of non-Newtonian fluids – Correlation of the laminar, transition, and turbulent-flow regions, AIChE J. 1 (1995) 434–440.
[28] A. Syrakos, Y. Dimakopoulos, J. Tsamopoulos, A finite volume method for the simulation of elastoviscoplastic flows and its application to the lid-driven cavity case, J. Non-Newtonian Fluid Mech. 275 (2020), 104216.
[29] D. Pasias, A. Passos, G. Constantinides, S. Balabani, E. Kaliviotis, Surface tension driven flow of blood in a rectangular microfluidic channel: effect of erythrocyte aggregation, in: Phys. Fluids, 32, 2020, 071903.